*Journal of The Electrochemical Society*, **155** (12) G295-G298 (2008)
0013-4651/2008/155(12)/G295/4/$23.00 © The Electrochemical Society


# High-Performance MIM Capacitors Using a High-κ TiZrO Dielectric

**C. H. Cheng,[a] H. C. Pan,[c] S. H. Lin,[d] H. H. Hsu,[a] C. N. Hsiao,[c] C. P. Chou,[a] F. S. Yeh,[d] and Albert Chin[b,z]**

[a]*Department of Mechanical Engineering and* [b]*Department of Electronics Engineering, National Chiao-Tung University, Hsinchu, Taiwan*
[c]*Instrument Technology Research Center, National Applied Research Labs, Hsinchu, Taiwan*
[d]*Department of Electrical Engineering, National Tsing Hua University, Hsinchu, Taiwan*

We have fabricated high-κ Ni/TiZrO/TaN metal–insulator–metal (MIM) capacitors. A low leakage current of $3.3 \times 10^{-8}$ A/cm$^2$ at −1 V was obtained for a 18 fF/μm$^2$ capacitance density. For a 5.5 fF/μm$^2$ capacitance density device, a small voltage coefficient of capacitance α of 105 ppm/V$^2$ and temperature coefficient of capacitance of 156 ppm/°C were measured.
 [DOI: 10.1149/1.2993977] 

Manuscript submitted July 2, 2008; revised manuscript received September 9, 2008. Published October 14, 2008.

The continuously increasing capacitance density ($\varepsilon_0\kappa/t_\kappa$) and preserving low leakage current are the technology trends of the metal–insulator–metal (MIM) capacitors.[1-18] To achieve this goal, the use of higher-κ dielectrics for MIM capacitors is required. However, the increasing κ value usually decreases the conduction band offset ($\Delta E_C$) to the metal electrode, where the $\Delta E_C$ even becomes slightly negative (−0.1 eV) in $SrTiO_3$ (STO).[18] Such a small $\Delta E_C$ increases the unwanted leakage current of MIM capacitors,[16] and therefore a trade-off between the $\Delta E_C$ and κ values is necessary. Besides, the κ value in STO is strongly dependent on the process temperature due to the formation of nanocrystals above 450°C.[16] Unfortunately, such a high temperature is above the maximum allowable temperature of 400°C for very large-scale integration (VLSI) back-end integration. In this paper, we report low leakage TiZrO MIM capacitors processed at 400°C. Using a low cost and high work function (5.1 eV) Ni electrode, low leakage currents of $3.3 \times 10^{-8}$ and $2.5 \times 10^{-7}$ A/cm$^2$ at, respectively, −1 and −2 V, were measured for the Ni/TiZrO/TaN MIM capacitors at 18 fF/μm$^2$ density. These electrical characteristics are better than previously reported for Ir/TiTaO/TaN[12,13] and Ni/TiHfO/TaN[15] capacitors with a close leakage current but at a slightly lower capacitance density of 14.3 fF/μm$^2$. Besides, a small quadratic voltage coefficient of capacitance (VCC α) of 105 ppm/V$^2$ and a temperature coefficient of capacitance (TCC) of 156 ppm/°C were measured in the 5.5 fF/μm$^2$ TiZrO MIM capacitor. Such excellent device characteristics are due to the higher $\Delta E_C$ for $ZrO_2$ (1.4 eV) than $Ta_2O_5$ (0.3 eV) and better κ of $ZrO_2$ than $HfO_2$.[19,20] These good device performances of Ni/TiZrO/TaN capacitors can be used for multiple functional system-on-chip (SoC) application.

## Experimental

The high-κ TiZrO MIM capacitors were fabricated on Si wafers. For VLSI back-end integration, a 2 μm thick $SiO_2$ isolation layer was first deposited on the Si substrates. After that, the combined bottom electrode of 200 nm Ta and then 50 nm TaN were deposited by sputtering. The TaN surface was exposed to a $NH_3^+$ plasma treatment to increase the oxidation resistance during the following post-deposition annealing (PDA).[5,6] Then, a 16, 47, or 56 nm thick $Ti_xZr_{1-x}O$ ($x \sim 0.67$) dielectric layer was deposited by physical vapor deposition (PVD). Because the as-deposited TiZrO by PVD at room temperature is highly defective, a 400°C PDA in oxygen ambient was performed to reduce the defects in TiZrO and leakage current.[3] This 400°C PDA is also used in the VLSI back-end-of-line to fabricate the MIM capacitors. From the PDA temperature-dependent X-ray diffraction analysis, the TiZrO maintained an amorphous phase even up to 450°C. Finally, a 40 nm Ni and/or 50 nm Al was deposited and patterned to form the top electrode. The metal thickness for both the top and bottom electrode should be as thin as possible for dynamic random access memory (DRAM) but relatively thick for radio-frequency (rf) application to decrease the series resistance. The bottom TaN was made thicker because of the larger resistivity. A large capacitor size of 180 × 180 μm was measured. The devices were characterized by capacitance-voltage (*C-V*) and current-voltage (*J-V*) measurements.

## Results and Discussion

Figures 1a and b show the *C-V* and *J-V* characteristics of Ni/TiZrO/TaN and Al/TiZrO/TaN capacitors. A high capacitance density of 18 fF/μm$^2$ was measured at 500 kHz. At −2 V, the leakage current of TiZrO MIM capacitors improves by 2 orders of magnitude using a high work function Ni (5.1 eV) as compared with Al (~4.1 eV) electrode. At this 18 fF/μm$^2$ capacitance density, low leakage currents of $3.3 \times 10^{-8}$ and $2.5 \times 10^{-7}$ A/cm$^2$ at −1 and −2 V were measured in a Ni/TiZrO/TaN MIM capacitor, respectively. Table I summarizes the device performance of various MIM capacitors. The Ni/TiZrO/TaN device data are better than those of the Ir/TiTaO/TaN MIM capacitors with a lower 14.3 fF/μm$^2$ capacitance density shown in Table I, even though a higher work function Ir top electrode (~5.27 eV) is used for the TiTaO capacitor than the Ni electrode (~5.1 eV) for TiZrO. This is mainly attributed to the larger conduction band offset of $ZrO_2$ (1.4 eV) than that of $Ta_2O_5$ (0.3 eV).[19] The device performance of Ni/TiZrO MIM capacitors is also better than the Ni/TiHfO,[15] where a higher capacitance density is obtained in Ni/TiZrO with a comparable leakage current shown in Table I. This is due to the higher κ for $ZrO_2$ than $HfO_2$ with close $\Delta E_C$, which is the reason why $ZrO_2$ is used in DRAM to replace $HfO_2$.[20] For analog integrated circuit (IC) application, a low VCC α is required. Figure 1c shows the $\Delta C/C$-$V$ characteristics of TiZrO MIM capacitors, where VCC α can be extracted from the following equation: $C(V) = C_0(\alpha V^2 + \beta V + 1)$; α and β are the quadratic and linear VCC, respectively. The VCC α is better using a Ni electrode than the Al. This may arise from the higher work function of Ni than Al, which exponentially decreases the free carrier injection from the electrode by Schottky emission and lowers the effect of charge relaxation.[21]

To further lower the VCC, we fabricated TiZrO dielectric capacitors at larger 47 and 56 nm thickness. Figures 2a-c show the *C-V*, *J-V*, and $\Delta C/C$-$V$ characteristics of Ni/TiZrO/TaN capacitors at these TiZrO thicknesses. Low leakage currents of $6.7 \times 10^{-8}$ and $4 \times 10^{-8}$ at −2 V were measured at a capacitance density of 6.5 and 5.5 fF/μm$^2$, respectively. Both the VCC α and β decrease with increasing TiZrO thickness or decreasing capacitance density. A small VCC α of 105 ppm/V$^2$ and a VCC β of −757 ppm/V at 500 kHz

[z] E-mail: albert_achin@hotmail.com

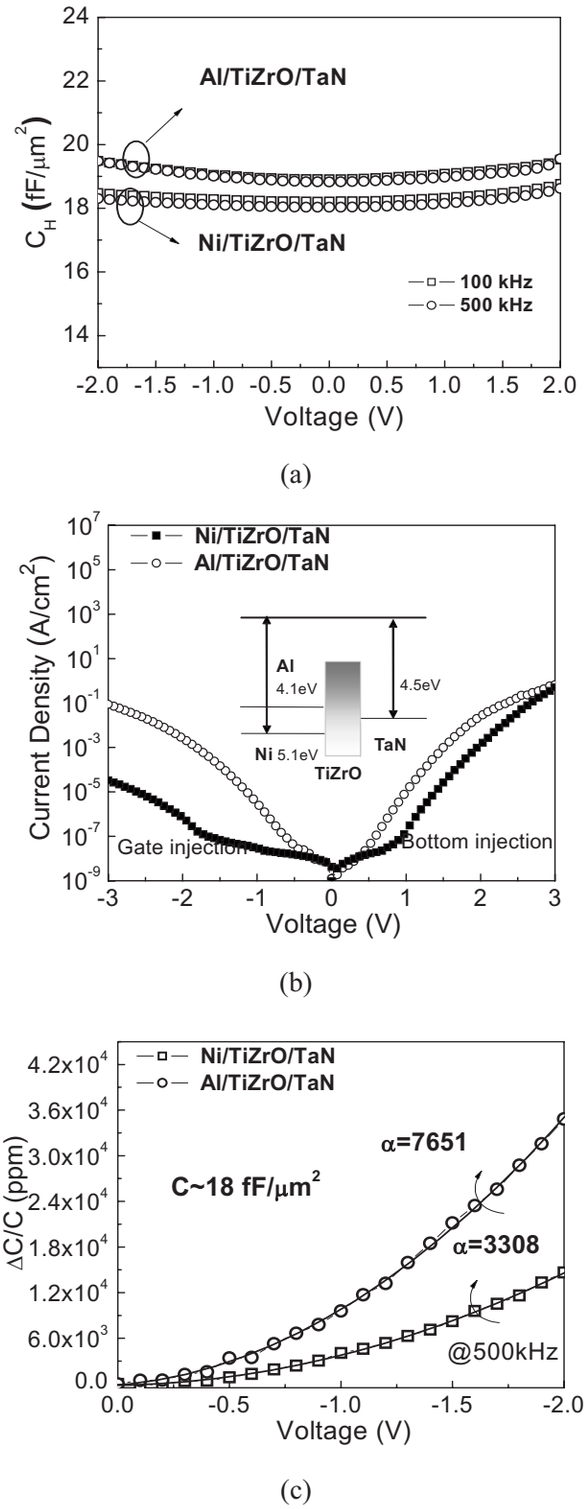


**Figure 1.** (a) *C-V*, (b) *J-V*, and (c) $\Delta C/C$-*V* characteristics of Al/TiZrO/TaN and Ni/TiZrO/TaN MIM capacitors.

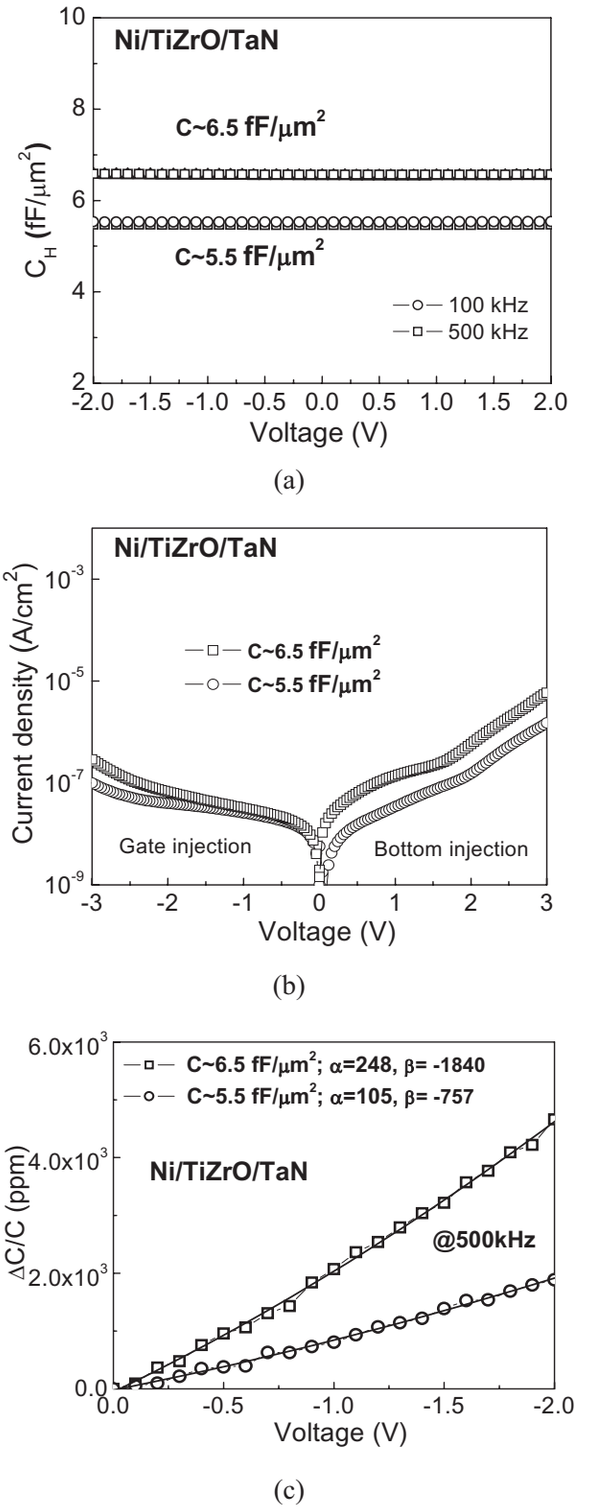


**Figure 2.** (a) *C-V*, (b) *J-V*, and (c) $\Delta C/C$-*V* characteristics of Ni/TiZrO/TaN MIM capacitors with 47 or 56 nm TiZrO dielectric thicknesses.

were obtained at a 56 nm thickness of TiZrO with a capacitance density of 5.5 fF/$\mu m^2$. Besides, the small dissipation factor from 0.015 to 0.084 was measured with increasing frequency from 10 to 500 kHz. These results indicate that the Ni/TiZrO/TaN capacitor is a good candidate for rf application. From the experimental data presented in Fig. 1c and 2c, the VCC $\alpha$ improves with increasing the metal work function and dielectric thickness, where both cases give the lower charge injection into the capacitor. This was well explained by the charge injection model reported previously.[21] These good device performances nearly meet the requirements of

**Table I. Comparison of MIM capacitors with various dielectrics and metal electrodes.**

| | $HfO_2$ [a] | Tb-$HfO_2$ [b] | TiTaO[c] | TiHfO[d] | ITRS@2012[e] | TiZrO[f] | | |
|---|---|---|---|---|---|---|---|---|
| Top electrode | Ta | Ta | Ir | Ni | — | Ni | | |
| Work-function (eV) | 4.2 | 4.2 | 5.27 | 5.1 | — | 5.1 | | |
| *C* Density (fF/μm$^2$) | 13 | 13.3 | 14.3 | 14.3 | 5 | 18 | 6.5 | 5.5 |
| *J* (A/cm$^2$) @25°C | $6 \times 10^{-7}$ (2 V) | $1 \times 10^{-7}$ (2 V) | $2 \times 10^{-7}$ (2 V) | $8.4 \times 10^{-8}$ (1 V) | — | $3.3 \times 10^{-8}$ (1 V) $2.5 \times 10^{-7}$ (2 V) | $6.7 \times 10^{-8}$ (2 V) | $4 \times 10^{-8}$ (2 V) |
| α (ppm/V$^2$) | 607 | 2667 | 634 | 3392 | $\alpha < 100$ | 3308 | 248 | 105 |
| TCC (ppm/°C) | — | 123 | — | 123 | — | — | 179 | 156 |

[a] Ref. [8]
[b] Ref. [10]
[c] Ref. [12,13]
[d] Ref. [15]
[e] Ref. [1]
[f] This work.

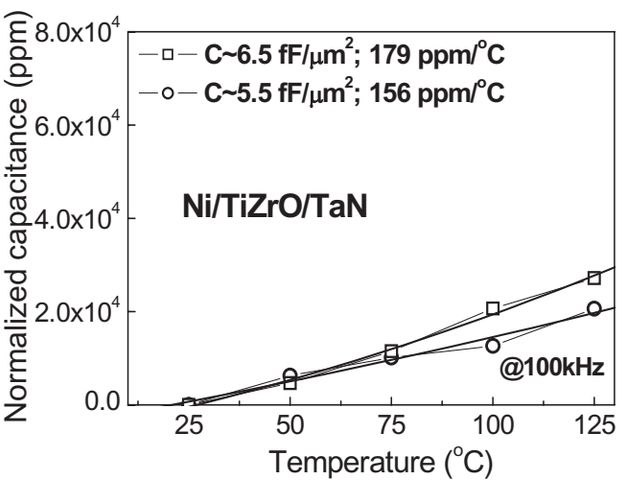


**Figure 3.** TCC characteristics of Ni/TiZrO/TaN MIM capacitors with 47 or 56 nm TiZrO dielectric thicknesses.

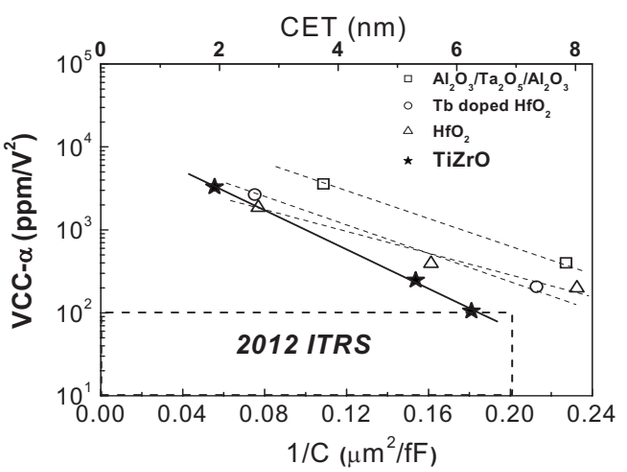


**Figure 4.** $\Delta C/C$-$1/C$ plot for various MIM capacitors.

bypass capacitors used for rf circuits listed in the International Technology Roadmap for Semiconductors (ITRS) for the year 2012, with a capacitance density >5 fF/μm$^2$, a VCC $|\alpha| < 100$ ppm/V$^2$, and a VCC $|\beta| < 1000$ ppm/V.[1]

The TCC is an important factor, because modern ICs usually operate at elevated temperatures. Figure 3 shows the measured normalized capacitance as a function of temperature. Small TCC values of 179 and 156 ppm/°C were measured at 100 kHz for the 6.5 and 5.5 fF/μm$^2$ density TiZrO MIM capacitors, respectively. The decreasing trend of TCC with decreasing capacitance density is similar to the VCC α case, which again may be related to the charge trapping and relaxation in MIM capacitors.[21]

Such an improving trend of VCC α with the decreasing capacitance density of MIM capacitors is summarized in Fig. 4. Here, the variation of α is plotted as a function of $1/C$ to show the dependence of capacitance equivalent thickness ($=\varepsilon_0\kappa/C$). The TiZrO shows a better chance to meet the ITRS requirement in 2012 than $HfO_2$ and $Ta_2O_5$. Besides, for the same required VCC $|\alpha| < 100$ ppm/V$^2$, the TiZrO can have a higher capacitance density than using $HfO_2$ and $Ta_2O_5$.

We have further studied the thermal stability of a Ni/TiZrO/TaN capacitor. Figures 5a and b display the *C*-*V* and *J*-*V* characteristics of a Ni/TiZrO/TaN device before and after thermal annealing at 350°C for 20 min under $N_2$ ambient. Only a small degradation of the capacitance density and leakage current was found, which indicates the good thermal stability of both the top Ni electrode and the TiZrO dielectric.

## Conclusions

We have investigated the device characteristics of Ni/TiZrO/TaN capacitors. A low leakage current and high capacitance density were obtained and better than previously reported MIM capacitors using a TiTaO or TiHfO dielectric. A low leakage current, a small VCC α of 105 ppm/V$^2$, and a TCC of 156 ppm/°C have been achieved in Ni/TiZrO/TaN MIM devices at 5.5 fF/μm$^2$ capacitance density. This high-performance device is capable of being integrated into a VLSI back-end and being used in multiple functions associated with SoC.

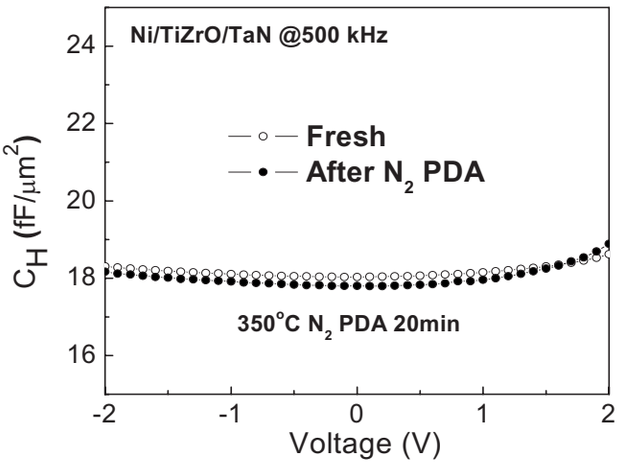


(a)

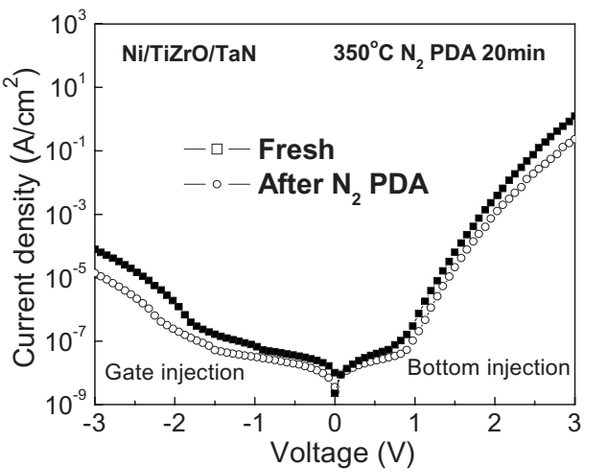


(b)

**Figure 5.** Thermal stability behavior of (a) *C-V* and (b) *J-V* characteristics for Ni/TiZrO/TaN capacitors after a 350°C $N_2$ anneal for 20 min.


## Acknowledgment

This work was supported in part by NSC 95-2221-E-009-275 of Taiwan.

*National Chiao-Tung University assisted in meeting the publication costs of this article.*


## References


1. *The International Technology Roadmap for Semiconductors: Semiconductor Industry Association*, 2005, www.itrs.net.
2. C.-M. Hung, Y.-C. Ho, I.-C. Wu, and K. O, *IEEE Trans. Microwave Theory Tech.*, **46**, 505 (1998).
3. J. A. Babcock, S. G. Balster, A. Pinto, C. Dirnecker, P. Steinmann, R. Jumpertz, and B. El-Kareh, *IEEE Electron Device Lett.*, **22**, 230 (2001).
4. C. H. Ng, K. W. Chew, and S. F. Chu, *IEEE Electron Device Lett.*, **24**, 506 (2003).
5. T. Ishikawa, D. Kodama, Y. Matsui, M. Hiratani, T. Furusawa, and D. Hisamoto, in *IEDM Technical Digest*, p. 940 (2002).
6. S. B. Chen, J. H. Lai, A. Chin, J. C. Hsieh, and J. Liu, *IEEE Electron Device Lett.*, **23**, 185 (2002).
7. S. B. Chen, J. H. Lai, K. T. Chan, A. Chin, J. C. Hsieh, and J. Liu, *IEEE Electron Device Lett.*, **23**, 203 (2002).
8. X. Yu, C. Zhu, H. Hu, A. Chin, M. F. Li, B. J. Cho, D.-L. Kwong, P. D. Foo, and M. B. Yu, *IEEE Electron Device Lett.*, **24**, 63 (2003).
9. H. Hu, S. J. Ding, H. F. Lim, C. Zhu, M. F. Li, S. J. Kim, X. F. Yu, J. H. Chen, Y. F. Yong, B. J. Cho, et al., in *IEDM Technical Digest*, p. 379 (2003).
10. S. J. Kim, B. J. Cho, M.-F. Li, C. Zhu, A. Chin, and D. L. Kwong, *Symposium on VLSI Technical Digest*, p. 77 (2003).
11. S. J. Kim, B. J. Cho, M. B. Yu, M.-F. Li, Y.-Z. Xiong, C. Zhu, A. Chin, and D. L. Kwong, in *Symposium on VLSI Technical Digest*, p. 56 (2005).
12. K. C. Chiang, A. Chin, C. H. Lai, W. J. Chen, C. F. Cheng, B. F. Hung, and C. C. Liao, in *Symposium on VLSI Technical Digest*, p. 62 (2005).
13. K. C. Chiang, C. H. Lai, A. Chin, T. J. Wang, H. F. Chiu, J. R. Chen, S. P. McAlister, and C. C. Chi, *IEEE Electron Device Lett.*, **26**, 728 (2005).
14. C. H. Cheng, H. C. Pan, H. J. Yang, C. N. Hsiao, C. P. Chou, S. P. McAlister, and A. Chin, *IEEE Electron Device Lett.*, **28**, 1095 (2007).
15. C. H. Cheng, K. C. Chiang, H. C. Pan, C. N. Hsiao, C. P. Chou, S. P. McAlister, and A. Chin, *Jpn. J. Appl. Phys., Part 1*, **46**, 7300 (2007).
16. K. C. Chiang, C. C. Huang, A. Chin, W. J. Chen, H. L. Kao, M. Hong, and J. Kwo, in *Symposium on VLSI Technical Digest*, p. 102 (2006).
17. K. C. Chiang, C. C. Huang, A. Chin, G. L. Chen, W. J. Chen, Y. H. Wu, A. Chin, and S. P. McAlister, *IEEE Trans. Electron Devices*, **53**, 2312 (2006).
18. K. C. Chiang, C. H. Cheng, H. C. Pan, C. N. Hsiao, C. P. Chou, A. Chin, and H. L. Hwang, *IEEE Electron Device Lett.*, **28**, 235 (2007).
19. J. Robertson, *J. Vac. Sci. Technol. B*, **18**, 1785 (2000).
20. K. Kim, in *IEDM Technical Digest*, p. 323 (2005).
21. C. Zhu, H. Hu, X. Yu, S. J. Kim, A. Chin, M. F. Li, B. J. Cho, and D. L. Kwong, in *IEDM Technical Digest*, p. 879 (2003).